Direct determination of absorption anisotropy in colloidal quantum rods

John Sundar Kamal,[1,2] Raquel Gomes,[1,2] Zeger Hens,[1,2,*] Masoumeh Karvar,[2,3] Kristiaan Neyts,[2,3] Sien Compernolle,[4] and Frank Vanhaecke[4]

[1]*Physics and Chemistry of Nanostructures, Ghent University, Krijgslaan 281-S3, B-9000 Gent, Belgium*

[2]*Center for Nano and Biophotonics, Ghent University, B-9000 Gent, Belgium*

[3]*Liquid Crystals and Photonics, Ghent University, Sint-Pietersnieuwstraat 46, B-9000 Gent, Belgium*

[4]*Department of Analytical Chemistry, Ghent University, Krijgslaan 281-S12, B-9000 Gent, Belgium*

(Received 7 November 2011; published 27 January 2012)

We propose a direct method to determine absorption anisotropy of colloidal quantum rods. In this method, the rods are aligned in solution by using an alternating electric field and we measure simultaneously the resulting average change in absorption. We show that a frequency window for the electric field exists in which the change in absorbance as a function of field strength can be analyzed in terms of the quantum-rod dipole moment and the absorption coefficient for light that is polarized parallel or perpendicular to the long axis of the rod. The approach is verified by measuring the absorbance change of CdSe rods at 400 nm as a function of field strength, where we demonstrate excellent agreement between experiment and theory. This enables us to propose improved values for the CdSe quantum-rod extinction coefficient. Next, we analyze CdSe/CdS dot-in-rods and find that the absorption of the first exciton transition is fully anisotropic, with a vanishing absorption coefficient for light that is polarized perpendicularly to the long axis of the rods.

DOI: 10.1103/PhysRevB.85.035126 PACS number(s): 78.67.−n, 42.25.Bs, 81.07.−b

I. INTRODUCTION

Progress in colloidal synthesis over the last 20 years has made available a wide range of metal, metal oxide, and semiconductor nanocrystals with an exceptional control over size, size dispersion, and shape.[1] Focusing on semiconductor nanocrystals, this involves, for example, spherical particles [quantum dots (QDs)],[2] rodlike particles [quantum rods (QRs)],[3] and heterostructures (core/shell, dot-in-rod).[4–6] This progress in synthesis is driven by the combination of optoelectronic properties tunable by size and shape, and versatile wet-chemical processing, which opens up a vast range of potential applications.[7] An important property of colloidal QDs is their absorption of light. The absorption spectrum reflects the quantized electronic energy levels of the QDs and it enables a quick quantification of the suspension in terms of QD size, size dispersion, and concentration. Moreover, as light absorption by a QD results in an electron/hole pair or exciton, they can be used as an absorber material in photodetectors and photovoltaic cells,[8–10] or as fluorophores, e.g., in biolabeling.[11]

Various literature studies confirm that the absorption coefficient μ of colloidal QDs can be understood within the framework of the Maxwell Garnett effective-medium theory. This implies that the screening of the electric field by the QD, as expressed by the local-field factor f_{LF}, is an essential factor determining μ (local-field approximation). Especially at photon energies considerably higher than that of the first exciton transition, experimental values agree with theoretical predictions using bulk dielectric constants.[12–17] The local-field approximation has also been applied to one-dimensional nanowires, where it predicts that μ takes different values for light that is polarized parallel ($\mu_{\parallel}$) and perpendicular ($\mu_{\perp}$) to the long axis of the wire. In the case of InP nanowires, the observation of polarized emission and emission excitation has been accordingly interpreted in terms of anisotropic local-field factors.[18] In addition, it has been shown for CdSe and CdTe nanowires that absorption anisotropy leads to an enhanced absorption coefficient even if the wires are randomly dispersed.[19,20] Rodlike colloidal semiconductor nanocrystals, either being homogeneous quantum rods (QRs) or heterogeneous dot-in-rods, combine the properties of both QDs and nanowires. Like QDs, they are considerably smaller than the wavelength of light, such that the local-field approximation applies, and, similar to nanowires, they have anisotropic optical properties.[21] Polarized emission and emission excitation have been demonstrated by single dot measurements on CdSe QRs[22] and CdSe/CdS dot-in-rods.[23] Opposite to the emission properties, experimental data on the absorption anisotropy of colloidal QRs and their possible correspondence to the predictions of the local-field approximation are rare. In the studies that address QR absorption, the local-field approximation is either assumed to hold[24] or the possibility of absorption anisotropy is not addressed.[25]

Here, we introduce an approach to determine absorption anisotropy on an ensemble of QRs. This is achieved by measuring the absorbance of a QR suspension, while aligning the rods simultaneously by means of an alternating electric field. We show that applying an electric field leads to a reduction of the absorbance, with an oscillation frequency twice that of the field. Moreover, a frequency window exists in which the absorbance reduction can be interpreted in terms of the QR dipole moment and anisotropic absorption coefficients. This approach is validated using CdSe QRs, where we find that the absorption anisotropy at short wavelengths corresponds to the predictions of the local-field approximation. This result is used to reassess the absorption coefficient of randomly dispersed QRs. In a next step, we extend the method to CdSe/CdS dot-in-rods, where we find that the ratio between the absorption coefficient that is perpendicular and parallel to the long axis of the rod is close to zero.

II. THEORETICAL BACKGROUND

The absorbance A of a QD dispersion can be quantified by the intrinsic absorption coefficient μ_i. With L as the length of the sample along the propagation direction of light, and f as the QD volume fraction, it reads

$$\mu_i = \ln 10 \frac{A}{fL}. \quad (1)$$

Apart from the factor $\ln 10$, μ_i gives the absorbance per unit length and per volume fraction of the QD material. For QDs like InAs,[13] wz- and zb-CdSe,[12,17] PbS,[14] PbSe,[16] and ZnO,[15] it has been shown that μ_i is independent of the QD size at energies well above the band-gap energy. Within the Maxwell Garnett model, the absorption coefficient can be written in terms of the refractive index n_s of the solvent and the dielectric function $\varepsilon = \varepsilon_R + i\varepsilon_I$ of the dispersed particles:[26]

$$\mu_{i,th} = \frac{2\pi\varepsilon_I}{n_s\lambda}|f_{LF}|^2. \quad (2)$$

Using the dielectric function for the corresponding bulk material generally leads to a good agreement between experimental and theoretical absorption coefficients for dispersed QDs at photon energies well above the energy of the first exciton transition.[12–17]

In Eq. (2), the local-field factor f_{LF} gives the ratio between the (optical) electric field outside (E_0) and inside (E) a QD. With α as the depolarization factor of the QD, and ε_s as the square of n_s, f_{LF} reads

$$f_{LF} = \frac{\varepsilon_s}{(1-\alpha)\varepsilon_s + \alpha\varepsilon}. \quad (3)$$

Equation (2) shows that $\mu_{i,th}$ strongly depends on $|f_{LF}|$, i.e., on the screening of the external field by the QD. With spherical objects, the depolarization factor is isotropic, amounting to $1/3$ regardless of the direction of the electric field with respect to the particle. With anisotropic shapes, this is no longer true. Prolate spheroids, for instance, have different depolarization factors for fields that are parallel ($\alpha_\parallel$) and perpendicular ($\alpha_\perp$) to their long axis. As shown in Fig. 1, this results in a different screening of parallel and perpendicular fields and thus different local-field factors, $f_{LF,\parallel}$ and $f_{LF,\perp}$. Therefore, the absorption coefficient will depend on the angle θ between the external (optical) electric field and the long axis of the spheroid (see Fig. 1):

$$\mu_{i,th} = \frac{2\pi\varepsilon_I}{n_s\lambda}|f_{LF,\parallel}|^2\cos^2\theta + \frac{2\pi\varepsilon_I}{n_s\lambda}|f_{LF,\perp}|^2\sin^2\theta. \quad (4)$$

According to Eq. (3), f_{LF} increases when α goes down if $\varepsilon > \varepsilon_s$, which is a typical situation for semiconductor nanocrystals in an apolar solvent. Hence, for a prolate spheroid, $f_{LF,\parallel}$ will be larger than $f_{LF,\perp}$,[27] implying an increase of the absorbance for optical electric fields that are parallel to the long axis, and a reduction for perpendicular fields.

III. EXPERIMENT

To determine the absorption coefficient anisotropy of colloidal quantum rods, we use a setup where a QR dispersion is sandwiched between two parallel, transparent electrodes. In this way, the absorbance of the dispersion can be measured as a function of an electric field—used to align the QRs—applied across this cell (see Fig. 2). In practice, the cell is constructed by two glass plates coated with indium tin oxide (ITO) on one side and held together with a glue containing 16 μm spacers. For each cell, the actual distance d between the electrodes is determined by interferometry. The optical cell is placed in an ultraviolet-visible (UV-vis) spectrophotometer (Perkin-Elmer lambda 35) and the absorbance is measured at a wavelength of 400 nm and at the first exciton peak. As the sampling rate of the spectrophotometer is 0.1 s, we either use low-frequency alternating fields, and measure the actual absorbance as a function of time, or high-frequency fields (0.5–10 kHz), leading to a measured absorbance which is a time average over many periods of oscillation.

The QRs that are used have been synthesized according to established literature recipes (see Supplemental Material, Information I)[28] and are dispersed after purification in dodecane for the absorbance measurements. To validate our experimental approach, we use CdSe QRs with an average length l of 33.6 nm, a diameter d of 8.9 nm, and an aspect ratio β of 3.8 (sample S5). For the measurements on CdSe/CdS dot-in-rods, we have used three different samples with aspect

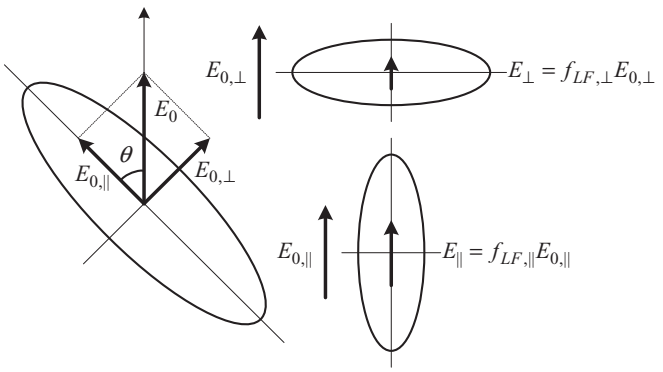

FIG. 1. A spheroid will screen the components of the external electric field E_0 that is parallel ($E_{0,\parallel}$) and perpendicular ($E_{0,\perp}$) to its long axis in a different way. This leads to different internal fields, $E_\parallel = f_{LF,\parallel}E_{0,\parallel}$ and $E_\perp = f_{LF,\perp}E_{0,\perp}$, and therefore different absorption coefficients (in the case of $\varepsilon > \varepsilon_s$).

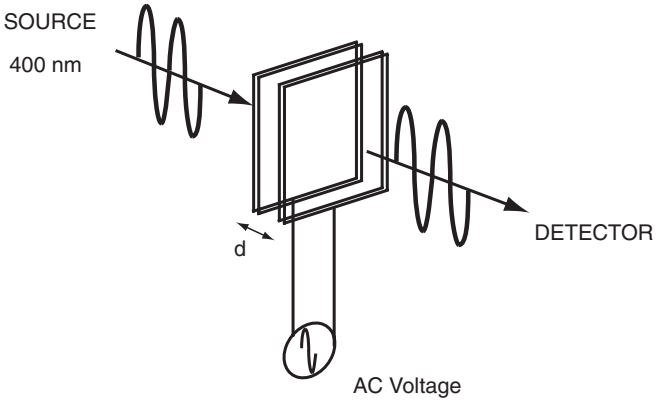

FIG. 2. Representation of the experimental setup consisting of an optical cell composed of two indium tin oxide (ITO)-coated glass plates separated by $d = 16$ μm spacers. The cell can be subjected to an ac voltage and is housed in a UV-vis spectrophotometer.

ratios $\beta = 3.2$ (sample S7), 4.3 (sample S6) and 4.8 (sample S8). Overview transmission electron microscopy images and the absorption spectra of the different samples used are given in the Supplemental Material, Information I.[28]

IV. RESULTS AND DISCUSSION

A. Method validation using CdSe QRs

1. Low-frequency ac field measurement

Figure 3 shows the change in absorbance of sample S5 when an ac field with a frequency f of 50 mHz and an amplitude E of 0.3 kV/cm is applied over a dispersion of CdSe QRs in dodecane. Two important observations follow from this experiment. First, with the electric field applied, the absorbance is always lower than the absorbance without the electric field. Second, the absorbance changes at a frequency of $2f$. Both observations are in line with the idea that (a) the electric field aligns the QRs with their long axis parallel to the field and (b) the measured change in absorbance reflects the orientation dependence of the QR absorption coefficient. Indeed, with the electric field applied along the propagation direction of the light, QRs align themselves with their long axis perpendicular to the optical electric field. As $f_{LF,\parallel} > f_{LF,\perp}$ for a prolate spheroid in a low dielectric constant environment, this leads to a reduction of the absorbance. In addition, the QR absorbance only depends on the angle θ between its long axis and the optical electric field. Therefore, the change in absorbance may depend on the magnitude of the electric field, but not on its sign. As a result, the absorbance oscillates at the double frequency of the electric field.

To corroborate the link between the absorbance changes and the alignment of the QRs, we further studied A as a function of E. For this purpose, low-frequency fields are not ideal. As shown before, even in dodecane, a fraction of the QRs carries an electric charge, implying that an applied electric field induces drift of the QRs toward the electrodes.[29] To prevent accumulation of the QRs at the electrodes, the period of oscillation should be shorter than the cell transit time, $\tau_{tr} = d/\mu E$, i.e., the time it takes for a single rod with mobility μ to cross the cell. For the S5 rods in a 16 μm cell, the cell transit time is about 10 ms for fields of 50 kV/cm. Therefore, we switch to higher frequency fields (0.5–10 kHz) to measure the average $\langle A \rangle$ of the absorbance.

2. Frequency dependence

Figure 4 shows $\langle |\Delta A|/A(0) \rangle$ measured on sample S4 as a function of f, keeping E constant at 96.8 kV/cm. One sees that with increasing frequency, the response strongly drops once the frequency exceeds 20 kHz. This drop can be understood by considering the rotational relaxation time $\tau_{\rm rot}$ of the rods about their short axis. Within the Debye-Perrin[30] model, $\tau_{\rm rot}$ is expressed as

$$\tau_{\rm rot} = \frac{C}{2k_B T}. \tag{5}$$

Here, k_B is the Boltzmann constant, T is the absolute temperature, and C is the rotational friction coefficient, which, for a prolate spheroid, reads

$$C = \frac{32\pi\eta}{3}\frac{a^4 - b^4}{(2a^2 - b^2)S - 2a}. \tag{6}$$

In this expression, η represents the viscosity of the solvent, while a and b stand for the the length of the minor and major half axis of the spheroid, respectively. The quantity S is linked to a and b according to

$$S = \frac{2}{(\sqrt{a^2 - b^2})}\ln\frac{a + \sqrt{a^2 - b^2}}{b}. \tag{7}$$

Taking a ligand shell thickness of 2 nm, the relaxation time $\tau_{\rm rot}$ calculated for the QRs used here amounts to 3.6 μs (sample S4) and 7.3 μs (sample S5), respectively. This results in a critical frequency $1/2\pi\tau_{\rm rot}$ of 45 and 22 kHz, respectively. The value of 45 kHz for sample S4 corresponds reasonably well with the observed drop in $\langle |\Delta A|/A(0) \rangle$ at frequencies above 20 kHz. Hence, to ensure that the alignment of the QRs follows the applied ac field, the applied frequency should be smaller than $1/\tau_{\rm rot}$. This means that the quantitative analysis of absorption changes is limited to ac frequencies between $1/\tau_{tr}$ and $1/\tau_{\rm rot}$.

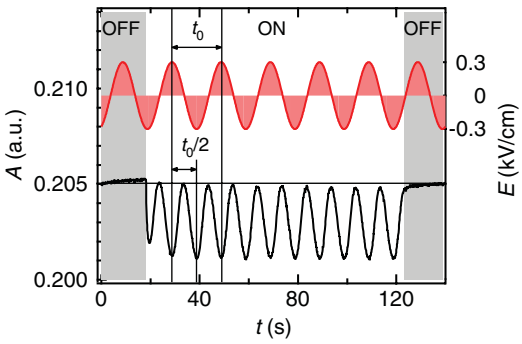

FIG. 3. (Color online) Top trace: Representation of the 50 mHz oscillating electric field applied over a dispersion of QRs. The time t_0 corresponds to 20 s. Bottom trace: Resulting change in absorbance measured with 3.8-aspect-ratio CdSe QRs.

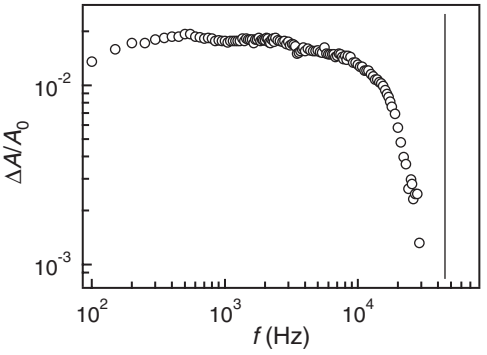

FIG. 4. Relative shift in absorbance measured as a function of the frequency f of the aligning field using a constant amplitude E of 96.8 kV/cm. The vertical line is drawn at 45 kHz, corresponding to $1/2\pi\tau_{\rm rot}$ for the sample analyzed here (S4).

3. High-frequency ac field measurement

Figure 5(a) shows a time trace of $\langle A \rangle$ when an 800 Hz electric field with amplitudes as indicated is switched on and off as a function of time. In line with the previous measurements (Fig. 3), we find that the absorbance drops upon application of an electric field, with a higher electric field yielding a larger change of the absorbance. In Fig. 5(b), the effect of an electric field on the QR absorbance is plotted more quantitatively as $\langle |\Delta A|/A(0) \rangle$ vs E. An element worth noticing here is that while the overall trend is an increase of $\langle |\Delta A|/A(0) \rangle$ with E, we find that at low field strengths, the slope $d\langle |\Delta A|/A(0) \rangle / dE$ tends to zero.

For ac fields with $f \gg 1/\tau_{tr}$, accumulation of the rods at the electrodes can be neglected. Hence, as long as f is sufficiently smaller than $1/2\pi\tau_{\rm rot}$, we can presume that the rods align according to Boltzmann statistics. In that case, an analytic expression for the absorption coefficient of an ensemble of QRs as a function of E can be obtained (see Supplemental Material, Information II).[28] Writing the ratio pE/k_BT, with p as the QR dipole moment, as $\mathcal{E}$, it reads

$$\mu_i = \mu_{i,\perp} + (\mu_{i,\parallel} - \mu_{i,\perp}) \left[\frac{\cosh(\mathcal{E})}{\mathcal{E}\sinh(\mathcal{E})} - \frac{1}{\mathcal{E}^2} \right]. \tag{8}$$

Here, the absorption coefficients for light that is polarized parallel and perpendicular to the long axis of the rod are defined as [see Eq. (4)]

$$\mu_{i,\parallel} = \frac{2\pi\varepsilon_I}{n_s\lambda} |f_{LF,\parallel}|^2, \tag{9}$$

$$\mu_{i,\perp} = \frac{2\pi\varepsilon_I}{n_s\lambda} |f_{LF,\perp}|^2. \tag{10}$$

Based on Eq. (8), we can calculate $\langle |\Delta A|/A(0) \rangle$, provided that $\mu_{i,\perp}$, $\mu_{i,\parallel}$ and p are known. Using the bulk dielectric function of wz-CdSe, this leaves us with the QR dipole moment as the only adjustable parameter. The full line in Fig. 5(b) represents the predicted values for $\langle |\Delta A|/A(0) \rangle$, using a dipole moment of $1.1\,10^{-27}$ C m, i.e., 330 D. This value is fully in line with published literature data,[31] which confirms that CdSe QRs have anisotropic absorption coefficients that can be understood simply from the anisotropy of the local-field factors.

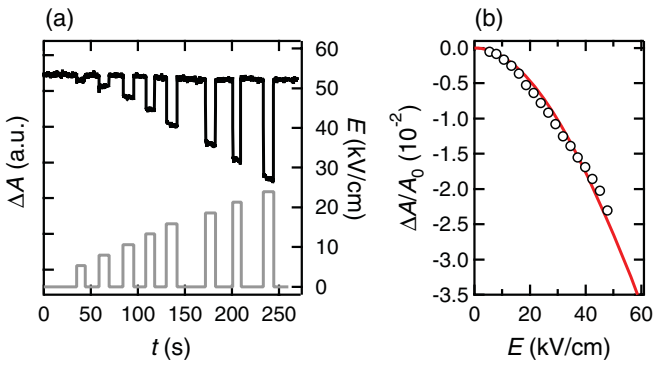

FIG. 5. (Color online) (a) Bottom trace: Amplitude of an 800 Hz electric field applied over a QR dispersion (S5). Top trace: Resulting change of the absorbance. (b) Resulting relative change of the absorbance as a function of field strength (symbols) and predicted change of $\langle |\Delta A|/A(0) \rangle$, according to Eq. (8), using a dipole moment of 333 D (solid line).

4. Assessment of the method

The excellent agreement between experiment and theory obtained with a realistic value of the QR dipole moment demonstrates that the approach presented here enables a direct measurement of absorption anisotropy of colloidal QRs. The quantitative analysis of $\langle |\Delta A|/A(0) \rangle$ as a function of E depends on two parameters, i.e., the dipole moment p and the ratio $\gamma = \mu_{i,\perp}/\mu_{i,\parallel}$ between the perpendicular and the parallel absorption coefficients. At high field strengths, $\langle |\Delta A|/A(0) \rangle$ reaches a limiting value that only depends on γ:

$$\lim_{E\to\infty} \left\langle \frac{|\Delta A|}{A(0)} \right\rangle = \frac{1-\gamma}{1+2\gamma}. \tag{11}$$

This means that in principle, both p and γ can be reliably determined by the experimental method proposed here. For CdSe QRs with an aspect ratio of 3.8, the limiting value of γ amounts to about 0.5. However, for the highest field strengths used here, for which pE is about equal to thermal energy, a relative change in absorbance of only 2–3% is predicted and measured. This means that the experiment in Fig. 5(b) only shows the beginning of the absorbance change, and in this case p and γ cannot be reliably determined together from a single trace. Increasing the field strength is difficult. It reduces τ_{tr}, which leads to irreversible changes of the absorbance with time. This limits the quantitative analysis to a situation where either p or γ are known. Interestingly, with the 50 mHz field used in Fig. 3, an absorbance drop by 2–3 % is achieved with considerably lower field strengths. Since, in this case, $f \ll 1/\tau_{tr}$, this may reflect the much stronger alignment of the CdSe QRs at the electrodes.[4]

B. The absorption coefficient of dispersed CdSe QRs

Equation (4) shows that the intrinsic absorption coefficient $\mu_{i,0}$ of randomly aligned QRs is a weighted average over $\mu_{i,\perp}$ and $\mu_{i,\parallel}$ (see Supplemental Material, Information II):[28]

$$\mu_{i,0} = \tfrac{2}{3}\mu_{i,\perp} + \tfrac{1}{3}\mu_{i,\parallel}. \tag{12}$$

Hence, opposite to colloidal QDs, the intrinsic absorption coefficient of QRs is not a constant, yet it depends on the aspect ratio of the rods. This also implies that QRs do not have the same intrinsic absorption coefficient as QDs, which can be considered as QRs with an aspect ratio of one. To verify this, we synthesized CdSe QR samples with four different aspect ratios and combined TEM imaging with elemental analysis by inductively coupled mass spectrometry. In this way, we could calculate the volume fraction of QRs in solution, and therefore obtain $\mu_{i,0}$ from the absorbance measured (see Supplemental Material, Information IV).[28] In Fig. 6(a), the line with the symbols shows $\mu_{i,0}$, thus determined for QRs with an aspect ratio $\beta = 3.6$ ($\beta = 3.6$ QRs) dispersed in heptane, next to theoretical curves calculated using the bulk dielectric function of wz-CdSe for QDs (gray background) and $\beta = 3.6$ QRs (solid line). We see that at wavelengths below 500 nm, the experimental $\mu_{i,0}$ exceeds the theoretical curve of wz-CdSe QDs and coincides with the theoretical $\mu_{i,0}$ of $\beta = 3.6$ QRs at wavelengths of about 300 nm. Figure 6(b) shows a comparison between the theoretical and experimental $\mu_{i,0}$ values at 300 nm of QRs with different aspect ratios. Despite the scatter on

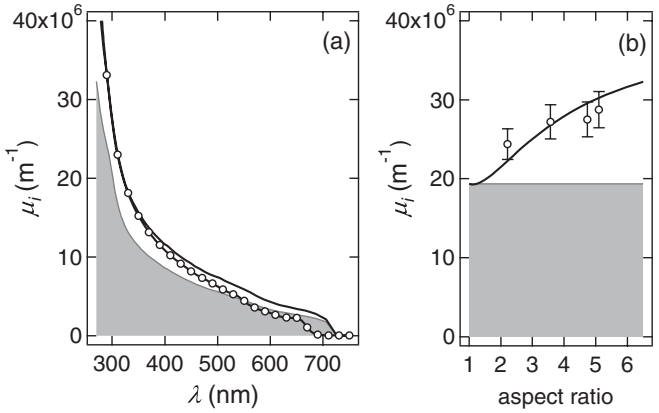

FIG. 6. (a) Spectrum of the intrinsic absorption $\mu_{i,0}$ for 3.6-aspect-ratio wz-CdSe QRs in heptane (sample S4) (line with symbols). Theoretical $\mu_{i,0}$ of 3.6-aspect-ratio wz-CdSe QRs in heptane (solid line), and theoretical $\mu_{i,0}$ of wz-QDs in heptane (gray background). (b) Experimentally determined $\mu_{i,0}$ at 300 nm for CdSe QR in heptane (samples S1–S4) (symbols). Theoretical $\mu_{i,0}$ of wz-CdSe QRs in heptane at 300 nm (solid line), and for wz-CdSe QDs (gray background).

the experimental values, the data show that the experimental $\mu_{i,0}$ of the QRs exceed the value of QDs by 21% to 43% for aspect ratios increasing from 2.3 to 5.4. Moreover, the experimental values largely coincide with the $\mu_{i,0}$ calculated for QRs using Eq. (12). In contrast with existing literature, we therefore conclude that the intrinsic absorption coefficient of colloidal QRs is not a constant equal to that of colloidal QDs of the same material.[25] Due to the anisotropy of the local-field factors, it markedly increases with increasing β, making QRs, in general, stronger absorbers than QDs. A similar conclusion followed from the analysis of the absorption coefficient of CdSe nanowires.[20]

C. Absorption anisotropy of CdSe/CdS dot-in-rods

CdSe/CdS dot-in-rods feature a spherical CdSe quantum dot enclosed in a CdS rod. In the literature, it has been assumed that this results in a fully anisotropic, first exciton transition.[32] To determine this anisotropy from the change of the first exciton absorbance with the applied field, the dipole moment of these dot-in-rods must be known. Therefore, we first measure $\langle|\Delta A|/A(0)\rangle$ at short wavelengths, where γ can be calculated using bulk optical constants.

Figures 7(a), 7(c), and 7(e) show $\langle|\Delta A|/A(0)\rangle$ at 400 nm as a function of field strength for CdSe/CdS dot-in-rods with aspect ratios of 3.2 (sample S7), 4.3 (sample S6), and 4.8 (sample S8), respectively. In all cases, the measured variation is highly similar to that of the CdSe QRs shown in Fig. 5(b). Using γ values calculated using the bulk optical constants of wurtzite CdS, an excellent correspondence of the experimental data and Eq. (8) is found for dipole moments of 117, 174, and 252 D, respectively.

At the first exciton transition, a similar decrease of $\langle|\Delta A|/A(0)\rangle$ with increasing field strength is observed for each of the samples, yet its magnitude is 1.5 to 2.5 times larger than at short wavelengths [Fig. 7(b)]. Since the dipole moment is the same at short and at long wavelengths, this implies that the

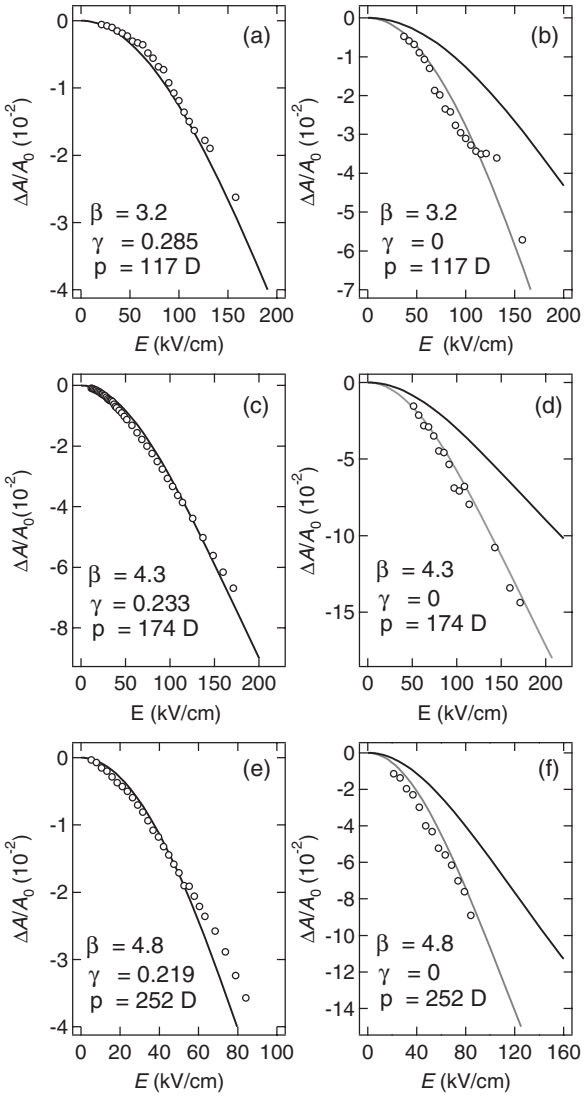

FIG. 7. (a) Resulting relative change of the absorbance as a function of field strength (symbols), and calculated change of $\langle|\Delta A|/A(0)\rangle$, according to Eq. (8), for $p = 117$ D and $\gamma = 0.285$ at 400 nm for CdSe/CdS dot-in-rods with an aspect ratio β of 3.2 (black line). (b) Relative change of the absorbance at the band edge (symbols), calculated change using the same values for p and γ as in (a) (black line), and calculated change taking $p = 117$ D and $\gamma = 0$ (gray line). (c),(d) The same as (a) and (b) for CdSe/CdS dot-in-rods with $\beta = 4.3$. (e),(f) The same as (a) and (b) for CdSe/CdS dot-in-rods with $\beta = 4.8$.

absorption anisotropy is considerably larger at the first exciton transition. In fact, for all samples, excellent quantitative agreement between the measurements and Eq. (8) is obtained by keeping the dipole moment fixed and taking $\gamma = 0$, which indicates that $\mu_\perp \ll \mu_\parallel$ at the band-gap transition.

For absorbers dispersed in a medium with refractive index n_s, the energy-integrated-absorption cross section $\sigma_{if,\mathrm{eV}}$ (which corresponds in the case of a QD or a QR to the product of the absorption coefficient and the QD or QR volume) of an electronic transition between an initial state $|i\rangle$ and a final state $|f\rangle$ is given by[33] (e, charge on the electron; ω, angular frequency of the incident light; ϵ_0, permittivity of the vacuum;

c, speed of light; **e**, polarization vector of the incident light; **r**, position vector)

$$\sigma_{if,\mathrm{eV}} = \frac{e\pi\omega}{\epsilon_0 n_s c}|\langle f|\mathbf{e}\cdot\mathbf{r}|i\rangle|^2 f_{LF}^2. \quad (13)$$

One sees that two factors can lead to absorption anisotropy. First, anisotropic local-field factors will lead to a dependence of $\sigma_{if,\mathrm{eV}}$ on the orientation of the rod relative to the optical electric field. As shown here, this suffices to understand absorption anisotropy at short wavelengths for CdSe QRs or CdSe/CdS dot-in-rods. Second, the transition matrix element $\langle f|\mathbf{e}\cdot\mathbf{r}|i\rangle$ can be orientation dependent. Clearly, this additional source of anisotropy is needed to explain why the variation of $\langle|\Delta A|/A(0)\rangle$ with applied field strength at the band gap of the CdSe/CdS dot-in-rods can only be fitted by setting $\gamma = 0$. More precisely, defining the long axis of a QR as the z axis, the results obtained here show that $\langle f|z|i\rangle \gg \langle f|x|i\rangle$ for the band-gap transition of CdSe/CdS dot-in-rods.

V. CONCLUSIONS

We introduce and assess an experimental method to analyze absorption anisotropy of dispersed rodlike colloidal nanocrystals, in which the absorbance of the dispersion is measured while aligning the nanocrystals using an electric field. Using alternating electric fields that are high enough to prevent charge accumulation at the electrodes and low enough to ensure rotational relaxation, we demonstrate that the resulting change in absorbance as a function of field strength can be quantified by a model based on Boltzmann statistics. The method is validated using CdSe quantum rods, where we find a difference between the absorption coefficient at 400 nm for fields that are polarized parallel and perpendicular to the rod axis, which is fully in line with the predictions of the local-field approximation. The absorption anisotropy implies that randomly dispersed CdSe quantum rods have a larger absorption coefficient than CdSe quantum dots. Finally, using this method, we have analyzed absorption anisotropy at the first exciton transition of CdSe/CdS dot-in-rods. Based on a quantitative analysis of the absorption change as a function of field strength, we find that this absorption is almost fully polarized, with a vanishing absorption coefficient for fields that are polarized perpendicular to the long axis of the rods.

ACKNOWLEDGMENTS

The authors acknowledge the Belgian Science Policy Office (IAP 6.10, photonics@be), the FWO-Vlaanderen (Project No. G.0144.08), and EU-FP7 (Integrated Training Network Herodot) for funding this research.

*zeger.hens@ugent.be

[1] Y. Yin and A. P. Alivisatos, Nature (London) **437**, 664 (2005).
[2] C. B. Murray, C. R. Kagan, and M. G. Bawendi, Annu. Rev. Mater. Sci. **30**, 545 (2000).
[3] X. Peng, L. Manna, W. D. Yang, J. Wickham, E. Scher, A. Kadavanich, and A. P. Alivisatos, Nature (London) **404**, 59 (2000).
[4] L. Carbone, C. Nobile, M. De Giorgi, F. D. Sala, G. Morello, P. Pompa, M. Hytch, E. Snoeck, A. Fiore, I. R. Franchini, M. Nadasan, A. F. Silvestre, L. Chiodo, S. Kudera, R. Cingolani, R. Krahne, and L. Manna, Nano Lett. **7**, 2942 (2007).
[5] M. A. Hines and P. Guyot-Sionnest, J. Phys. Chem. **100**, 468 (1996).
[6] D. V. Talapin, I. Mekis, S. Gotzinger, A. Kornowski, O. Benson, and H. Weller, J. Phys. Chem. B **108**, 18826 (2004).
[7] D. V. Talapin, J. S. Lee, M. V. Kovalenko, and E. V. Shevchenko, Chem. Rev. **110**, 389 (2010).
[8] T. Rauch, M. Boeberl, S. F. Tedde, J. Fuerst, M. V. Kovalenko, G. Hesser, U. Lemmer, W. Heiss, and O. Hayden, Nature Photon. **3**, 332 (2009).
[9] P. V. Kamat, J. Phys. Chem. C **112**, 18737 (2008).
[10] S. A. McDonald, G. Konstantatos, S. G. Zhang, P. W. Cyr, E. J. D. Klem, L. Levina, and E. H. Sargent, Nature Mater. **4**, 138 (2005).
[11] I. L. Medintz, H. T. Uyeda, E. R. Goldman, and H. Mattoussi, Nature Mater. **4**, 435 (2005).
[12] C. A. Leatherdale, W. K. Woo, F. V. Mikulec, and M. G. Bawendi, J. Phys. Chem. B **106**, 7619 (2002).
[13] P. R. Yu, M. C. Beard, R. J. Ellingson, S. Ferrere, C. Curtis, J. Drexler, F. Luiszer, and A. J. Nozik, J. Phys. Chem. B **109**, 7084 (2005).
[14] I. Moreels, K. Lambert, D. Smeets, D. De Muynck, T. Nollet, J. C. Martins, F. Vanhaecke, A. Vantomme, C. Delerue, G. Allan, and Z. Hens, ACS Nano **3**, 3023 (2009).
[15] P. Lommens, K. Lambert, F. Loncke, D. De Muynck, T. Balkan, F. Vanhaecke, H. Vrielinck, F. Callens, and Z. Hens, ChemPhysChem. **9**, 484 (2008).
[16] I. Moreels, K. Lambert, D. De Muynck, F. Vanhaecke, D. Poelman, J. C. Martins, G. Allan, and Z. Hens, Chem. Mater. **19**, 6101 (2007).
[17] R. K. Capek, I. Moreels, K. Lambert, D. De Muynck, Q. Zhao, A. Vantomme, F. Vanhaecke, and Z. Hens, J. Phys. Chem. C **114**, 6371 (2010).
[18] J. Wang, M. S. Gudiksen, X. Duan, Y. Cui, and C. M. Lieber, Science **293**, 1455 (2001).
[19] V. Protasenko, D. Bacinello, and M. Kuno, J. Phys. Chem. B **110**, 25322 (2006).
[20] J. Giblin and M. Kuno, J. Phys. Chem. Lett. **1**, 3340 (2010).
[21] R. Krahne, G. Morello, A. Figuerola, C. Georgea, S. Dekaa, and L. Mannaa, Phys. Rep. **501**, 75 (2011).
[22] X. Chen, A. Nazzal, D. Goorskey, M. Xiao, Z. A. Peng, and X. Peng, Phys. Rev. B **64**, 245304 (2001).
[23] F. Pisanello, L. Martiradonna, G. Leménager, P. Spinicelli, A. Fiore, L. Manna, J. P. Hermier, R. Cingolani, E. Giacobino, M. De Vittorio, and A. Bramati, Appl. Phys. Lett. **96**, 033101 (2010).
[24] H. Htoon, J. A. Hollingworth, A. V. Malko, R. Dickerson, and V. I. Klimov, Appl. Phys. Lett. **82**, 4776 (2003).
[25] E. Shaviv, A. Salant, and U. Banin, ChemPhysChem. **10**, 1028 (2009).
[26] D. Ricard, M. Ghanassi, and M. C. Schanne-klein, Opt. Commun. **108**, 311 (1994).
[27] J. A. Osborn, Phys. Rev. **67**, 351 (1945).

[28]See Supplemental Material at http://link.aps.org/supplemental/10.1103/PhysRevB.85.035126 for details concerning synthesis and size determination, derivation of Eq. (5), and elemental analysis and absorption coefficients.
[29]M. Cirillo, F. Strubbe, K. Neyts, and Z. Hens, ACS Nano **5**, 1345 (2011).
[30]P. F. Perrin, J. Phys. Radium **10**, 497 (1934).
[31]L.-S. Li and A. P. Alivisatos, Phys. Rev. Lett. **90**, 097402 (2003).
[32]A. Sitt, A. Salant, G. Menagen, and U. Banin, Nano Lett. **11**, 2054 (2011).
[33]E. Merzbacher, *Quantum Mechanics* (Wiley, New York, 1970).